Human Molecular Genetics, 2022, Vol. 31, No. 4 499–509

https://doi.org/10.1093/hmg/ddab260
Advance Access Publication Date: 9 September 2021
General Article

GENERAL ARTICLE

CFTR corrector C17 is effective in muscular dystrophy, *in vivo* proof of concept in LGMDR3

Martina Scano[1,†], Alberto Benetollo[1], Leonardo Nogara[2], Michela Bondì[1], Francesco Dalla Barba[1], Michela Soardi[1], Sandra Furlan[3], Eylem Emek Akyurek[4], Paola Caccin[1], Marcello Carotti[1], Roberta Sacchetto[4], Bert Blaauw[1,2] and Dorianna Sandonà[1,*,‡]

[1]Department of Biomedical Sciences, University of Padova, Padova, Italy, [2]Venetian Institute of Molecular Medicine, University of Padova, Padova, Italy, [3]Neuroscience Institute – Italian National Research Council (CNR), Padova, Italy and [4]Department of Comparative Biomedicine and Food Science, University of Padova, Padova, Italy

*To whom correspondence should be addressed at: Department of Biomedical Sciences, University of Padova, Via U. Bassi 58/B, 35131 Padova, Italy. Tel: +39 0498276028; Fax: +39 0498276040; Email: dorianna.sandona@unipd.it

Abstract

Limb-girdle muscular dystrophy R3 (LGMDR3) is caused by mutations in the *SGCA* gene coding for α-sarcoglycan (SG). Together with β- γ- and δ-SG, α-SG forms a tetramer embedded in the dystrophin associated protein complex crucial for protecting the sarcolemma from mechanical stresses elicited by muscle contraction. Most LGMDR3 cases are due to missense mutations, which result in non-properly folded, even though potentially functional α-SG. These mutants are prematurely discarded by the cell quality control. Lacking one subunit, the SG-complex is disrupted. The resulting loss of function leads to sarcolemma instability, muscle fiber damage and progressive limb muscle weakness. LGMDR3 is severely disabling and, unfortunately, still incurable. Here, we propose the use of small molecules, belonging to the class of cystic fibrosis transmembrane regulator (CFTR) correctors, for recovering mutants of α-SG defective in folding and trafficking. Specifically, CFTR corrector C17 successfully rerouted the SG-complex containing the human R98H-α-SG to the sarcolemma of hind-limb muscles of a novel LGMDR3 murine model. Notably, the muscle force of the treated model animals was fully recovered. To our knowledge, this is the first time that a compound designated for cystic fibrosis is successfully tested in a muscular dystrophy and may represent a novel paradigm of treatment for LGMDR3 as well as different other indications in which a potentially functional protein is prematurely discarded as folding-defective. Furthermore, the use of small molecules for recovering the endogenous mutated SG has an evident advantage over complex procedures such as gene or cell transfer.

[†]Martina Scano, http://orcid.org/0000-0002-8761-1730
[‡]Dorianna Sandonà, http://orcid.org/0000-0002-9908-2442
Received: July 13, 2021. **Revised:** August 23, 2021. **Accepted:** September 2, 2021

Graphical Abstract

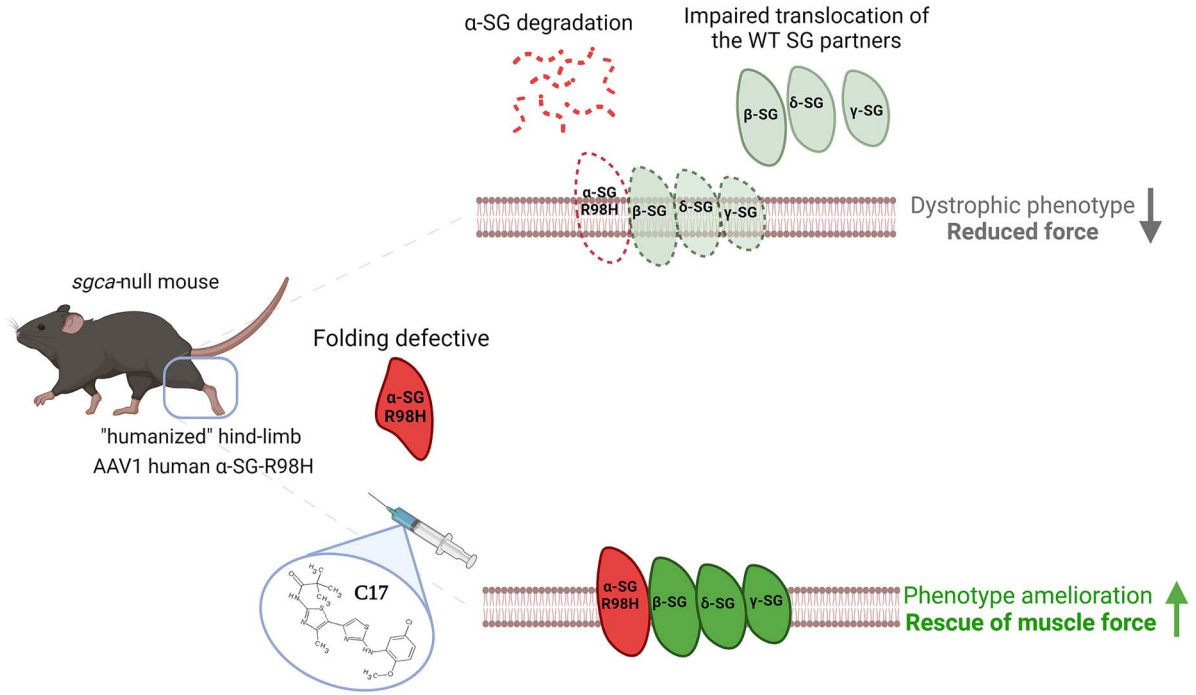

Introduction

LGMDR3, also known as LGMD2D or α-sarcoglycanopathy, is a rare autosomal recessive disease, affecting mainly the proximal limb musculature. The onset occurs in the childhood; it is progressive and very often forces the affected subjects to the wheel chair. Mild forms are also reported (1,2). The disease is caused by mutations of the *SGCA* gene coding for α-SG. Together with β-, γ- and δ-SG, α-SG forms a tetramer, which is part of the dystrophin associated protein complex and plays a major role in preserving sarcolemma from damage due to the repeated contractile mechanical stresses (2). The majority of the *SGCA* disease-causing defects are missense mutations and it has been observed that a single amino acid substitution may result in a folding defective α-SG, recognized by the quality control (QC) and delivered to the ubiquitin-proteasome system of the muscle cells for degradation (3–6). Consequently, the SG-complex is disrupted and unable to traffic to the membrane. This results in sarcolemma instability, muscle fiber damage and progressive muscle weakness (2). The disclosure of the molecular mechanism of the disease allowed the identification of potential novel druggable targets and notably evidenced that most of the mutants are still functional if prevented from being degraded (3,4,6–8). Like in LGMDR3, there are several other genetic diseases sharing a similar primary pathogenic event. Among them, there is cystic fibrosis (CF) when caused by class II mutations of the CF transmembrane regulator (CFTR) (9,10). Thus, we hypothesized that compounds able to recover CFTR mutants defective in folding and trafficking would have been active on α-SG too (11,12). Indeed, we have recently verified that small molecules, known as CFTR correctors, are effective in recovering missense mutants of α-SG in cellular models (13). More importantly, some of them promoted the rescue of the SG-complex in differentiated primary myogenic cells isolated from a LGMDR3 patient carrying the V247M/L31P mutations on the *SGCA* alleles. The rescued complex was stable and improved the sarcolemma integrity, even though containing a defective subunit (13,14). Here, we complete the study proving the efficacy of CFTR correctors *in vivo*, paying particular attention to muscle performance. Regrettably, the currently available SG knock in (KI) mice are unusable to this intent, as these animals do not develop a dystrophic phenotype (3,15,16). Therefore, we developed a novel model of the disease, in which the hind-limbs of the *sgca*-null mouse have been transduced by adeno associated viruses (AAV) expressing the human α-SG sequence carrying the R98H amino acid substitution. Thanks to these mice with humanized hind-limbs, we proved the efficacy of C17, the most promising CFTR corrector, previously identified (13,14). The myopathic phenotype significantly improved at both histological and molecular level and muscle force reached the level of that of healthy mice, upon 5 weeks of systemic administration of the small molecule. Notably, these ameliorations occurred in the absence of signs of toxicity.

Results

Generation and characterization of a mouse model of sarcoglycanopathy by hind-limbs humanization

First aim of this work was the generation of a novel murine model of LGMDR3 mirroring the human condition caused by a missense mutation in the *SGCA* gene. To this intent, we expressed the human α-SG sequence in the background of the *sgca*-null mouse by using the adeno associated virus serotype 1 (AAV1) (17,18). The virus was engineered to express the human α-SG carrying either the V247M or the R98H mutation (Supplementary Material, Fig. S1). As positive control, we prepared an AAV1 stock expressing the human wild type (WT) form of α-SG. The tMCK (modified muscle creatine kinase) tissue specific promoter assured the expression of the human protein in striated muscle (17,19).

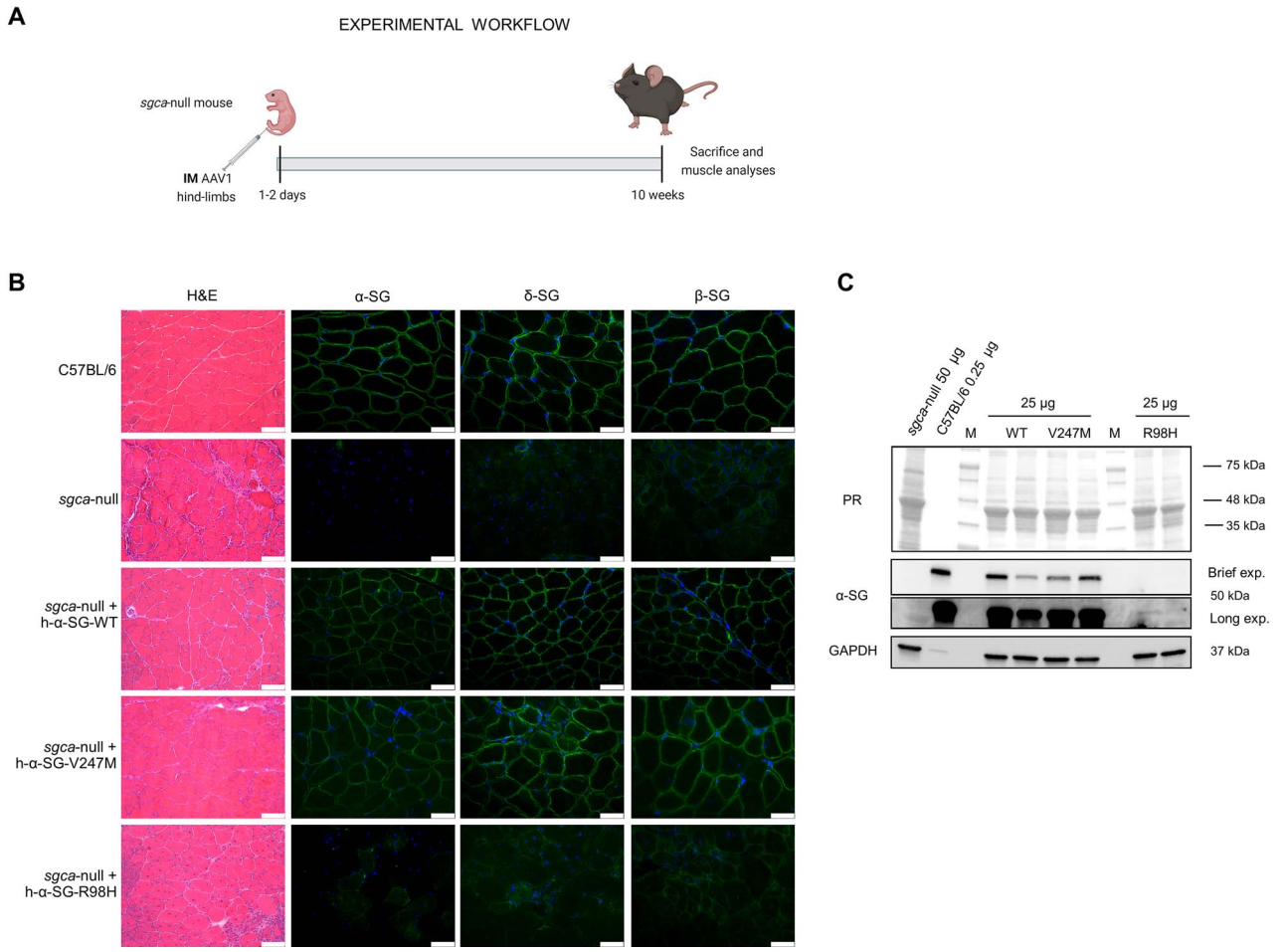

Figure 1. The LGMDR3 mouse model with humanized hind-limbs. (**A**) Scheme of the experimental work flow (created with BioRender.com). (**B**) Histological (H&E) and IF analyses of TA muscles cryo-sections from C57BL/6 (positive control), sgca-null (negative control) and sgca-null transduced with either the human WT α-SG sequence (*sgca*-null + h-α-SG-WT, positive control of transduction), the human V247M-α-SG sequence (*sgca*-null + h-α-SG-V247M) or the human R98H-α-SG sequence (*sgca*-null + h-α-SG-R98H). Primary antibodies specific for α-, δ- and β-SG, as indicated, were revealed by Alexa-Fluor488-conjugated secondary antibodies. IF images were captured at the same setting conditions. Bars correspond to 100 and 50 μm in H&E and IF images, respectively. (**C**) WB analysis of total protein lysates of representative TA muscle samples from negative and positive control (*sgca*-null and C57BL/6, respectively) and mice humanized with the different α-SG sequences, as indicated. The membrane was probed with primary antibodies to α-SG and GAPDH, used as loading control together with Ponceau Red protein staining. Two exposition-times of the α-SG-probed membrane are reported to appreciate the expression of the R98H mutant.

Animals were transduced by intramuscular injection of 9×10^9 viral genome (vg) of AAV1 in one hind-limb of 1 to 2-day-old *sgca*-null mouse pups; the contralateral leg, injected with physiological solution, was used as negative control. Ten weeks later, mice were sacrificed and the tibialis anterior (TA) muscle of the humanized hind-limbs further analyzed (Fig. 1A reports the strategy).

As expected, the expression of the human WT-α-SG sequence (positive control of transduction) resulted in the development of almost healthy phenotype with the sarcolemma localization of the SG-complex containing the human α-SG together with the endogenous partners, as proven by the immunofluorescence (IF) staining (Fig. 1B) (20).

Transduction with the mutated human α-SG sequences had a different outcome. Quite surprisingly, the presence of the V247M mutation did not result in the development of myopathic features because the whole SG-complex localized at the sarcolemma (Fig. 1B).

Conversely, the expression of the R98H-α-SG mutant led to the development of a dystrophic phenotype, with a clear variability in fiber size, nuclei internally located and inflammation. The α-SG immunoreactivity at the sarcolemma was extremely low, while traces of the protein were visible intracellularly in certain fibers. The surface localization of WT δ- and β-SG subunits resulted reduced, with much of the signal coming from within the fibers (Fig. 1B).

These findings were confirmed by western blot (WB) analysis of total protein lysates from TA muscle of the different mice (Fig. 1C). Indeed, α-SG was found in almost equal amount in muscles transduced with either WT or V247M human α-SG sequence, while a very low amount of R98H-α-SG was detected in muscle lysates. Of note, the amount of both WT- and V247M-α-SG protein was about 10 times lower in comparison to the level present in healthy, C57BL/6 mice.

C17 rescued the SG-complex at the sarcolemma of humanized mice expressing the R98H-α-SG mutant

As mice transduced with the human R98H-α-SG mimicked with high fidelity the human pathological condition, experiments aiming at validating the efficacy of corrector C17 *in vivo* were carried out in this humanized animal model. *Sgca*-null mouse

pups were transduced as above described in both hind-limbs. Seven weeks upon transduction, mice were treated systemically for 3 weeks by daily intraperitoneal injection (IP) of either corrector C17 or its vehicle (Fig. 2A reports the experimental workflow). Being hydrophobic, C17 was prepared in a vehicle comprising DMSO and the emulsifier Kolliphor EL (Supplementary Material, Fig. S2). The C17 dose of 25 mg/kg was chosen according to (21). We adopted the IP route of administration because it is minimally stressful in chronic treatments of small rodents and commonly used for proof-of-concept studies (22).

IF analysis (Fig. 2B) shows that C17 administration induced a strong α-SG localization at the sarcolemma; conversely, the signal was very low and partially confined intracellularly in vehicle-treated samples. Notably, there was an impressive rerouting at the sarcolemma of the δ-SG protein in treated versus control samples. The superimposable pattern of α- and δ-SG staining was the proof that the whole SG-complex was reconstituted at the sarcolemma upon C17 administration (23–25). Of note, the rerouting of the SG-complex at the surface of muscle fibers resulted in the amelioration of the histological phenotype of C17-treated samples. Indeed, the morphometric analysis of C17 versus vehicle-treated muscles showed a slight reduction in the number of small fibers, with the concomitant shift toward fibers with larger cross-sectional area (CSA) (Fig. 2C). The densitometric analysis of WB experiments (Supplementary Material, Fig. S3) of total protein lysates showed a tendency for the α-SG content to increase in C17-treated samples compared with vehicle-treated ones (Fig. 2D).

C17 induced muscle force recovery in humanized mice expressing the R98H-α-SG mutant in the absence of toxic effects

To investigate muscle function upon 5 weeks of C17 treatment (Fig. 3A reports the experimental workflow), the activity of TA muscles was evaluated by assessing force production *in vivo*, in response to nerve stimulation at different frequencies, according to (26,27). WT C57BL/6 and *sgca*-null mice of matching age and weight were tested as positive and negative control, respectively. As expected, in humanized animals with similar transgene copy number (Fig. 3B), the systemic administration of C17 promoted the proper localization of the SG-complex and the improvement of the myopathic phenotype (Fig. 3C). The comparison of the force/frequency curves of TA muscles from WT, *sgca*-null and vehicle- or C17-treated humanized mice, normalized for muscle weight, is reported in Fig. 3D. Notably, the muscle force generated by C17-treated mice (red line), since the single twitch (Supplementary Material, Fig. S4), is practically identical to that of WT (black line) and is significantly higher of the *sgca*-null mice force (light-blue line). This is a key result, showing the ability of corrector C17 in correcting the main phenotypic features of a muscular dystrophy and confirming all the data collected *in vitro* (13,14).

In Fig. 3D, it is also possible to observe that the muscle force generated by vehicle-treated humanized animals (blue line) was slightly higher, although not statistically significant, in comparison to the negative control animals (light-blue line).

The WB analysis of protein lysates from TA muscles allows appreciating that, besides the intrinsic variability of working with living animals, the C17-treated mice expressed a slightly higher amount of α-SG in comparison to the vehicle treated ones. As already observed (Fig. 1), the total amount of α-SG remained remarkably lower in humanized samples in comparison to WT mice (Fig. 3E).

In a few cases, like sample #3, we observed some α-SG expression in vehicle-treated animals. This seems not the result of a higher transduction rate. Indeed, the gene copy number (Fig. 3B) of this animal is lower than that of sample #2 that, conversely, presented a very low expression of the protein (Fig. 3E). On the other hand, α-SG of sample #3 did not better localize at the sarcolemma (Fig. 3C). Therefore, we suppose that sometimes, the α-SG mutant undergoes less efficient degradation by ERAD that, for unforeseen causes, in some animals may be less active.

Another essential point of this experiments is that animals treated for 5 weeks with C17 showed neither behavioral difference nor sign of distress in comparison to vehicle-treated mice; they grew at similar rate (Fig. 4A) reaching an average final weight of 23.63 ± 2.74 gr (C17 treated) and 23.90 ± 2.275 gr (vehicle treated). Furthermore, no major difference was observed at the histological level of kidneys and livers between vehicle- and C17-treated animals (Fig. 4B).

Discussion

Aim of the work here described is the *in vivo* validation of corrector C17 as potential therapeutic compound for LGMDR3, which is a severe muscular dystrophy belonging to the large family of rare diseases still without a cure. Our strategy is based on the knowledge that the molecular mechanism behind the majority of LGMDR3 and CF cases are similar (7,8,10,12). In both cases, missense mutations and small in frame deletions result in a folding defective protein impaired in trafficking to the final location that is recognized by the cell's QC and degraded by the ubiquitin-proteasome system (3–5,9). We therefore theorized that small molecules (CFTR correctors) rescuing class II mutants of CFTR could also have worked with α-SG mutants (11,12,28). Moreover, there is evidence collected *in vitro* that CFTR correctors may be effective on proteins different from CFTR (29–31). Our hypothesis was confirmed, as several CFTR correctors successfully rescued the SG-complex in cellular models and primary myogenic cells from a LGMDR3 patient (13,14). The *in vivo* validation of the most promising corrector was initially braked by the absence of a valuable animal model carrying a missense mutation in one of the *SGC* genes. Indeed, the available α-SG and β-SG KI mouse lines do not develop the dystrophic phenotype expected on the bases of the equivalent human mutations (3,15,16). Several explanations may be thought for the failure in reproducing the dystrophic phenotype of LGMDR3 and R4 in mouse, and further studies may be carried out related to the 3D structure of SGs and/or the QC and degradative systems. Nevertheless, to bypass this bottleneck, we adopted an alternative approach to generate a valuable model of LGMDR3. In the background of the *sgca*-null mouse, we induced the expression of the human α-SG carrying either the V247M or the R98H missense mutation by exploiting the transduction via AAV. Transduction was limited to the hind-limbs and was performed in new-born mice to assure tolerance toward the human protein and the development and growth of the muscle in the presence of the mutated SG. The use of AAV1 and the tMCK promoter to assure efficient delivery and controlled skeletal muscle expression of the human α-SG protein was previously well documented, evidencing a long persistence, up to one year, of the transgenic protein (17–20). It is also well known that *sgca*-null mice develop a progressive muscular dystrophy starting 1 week upon birth and becoming highly severe at 2 months of age (32,33). However, we transduced human

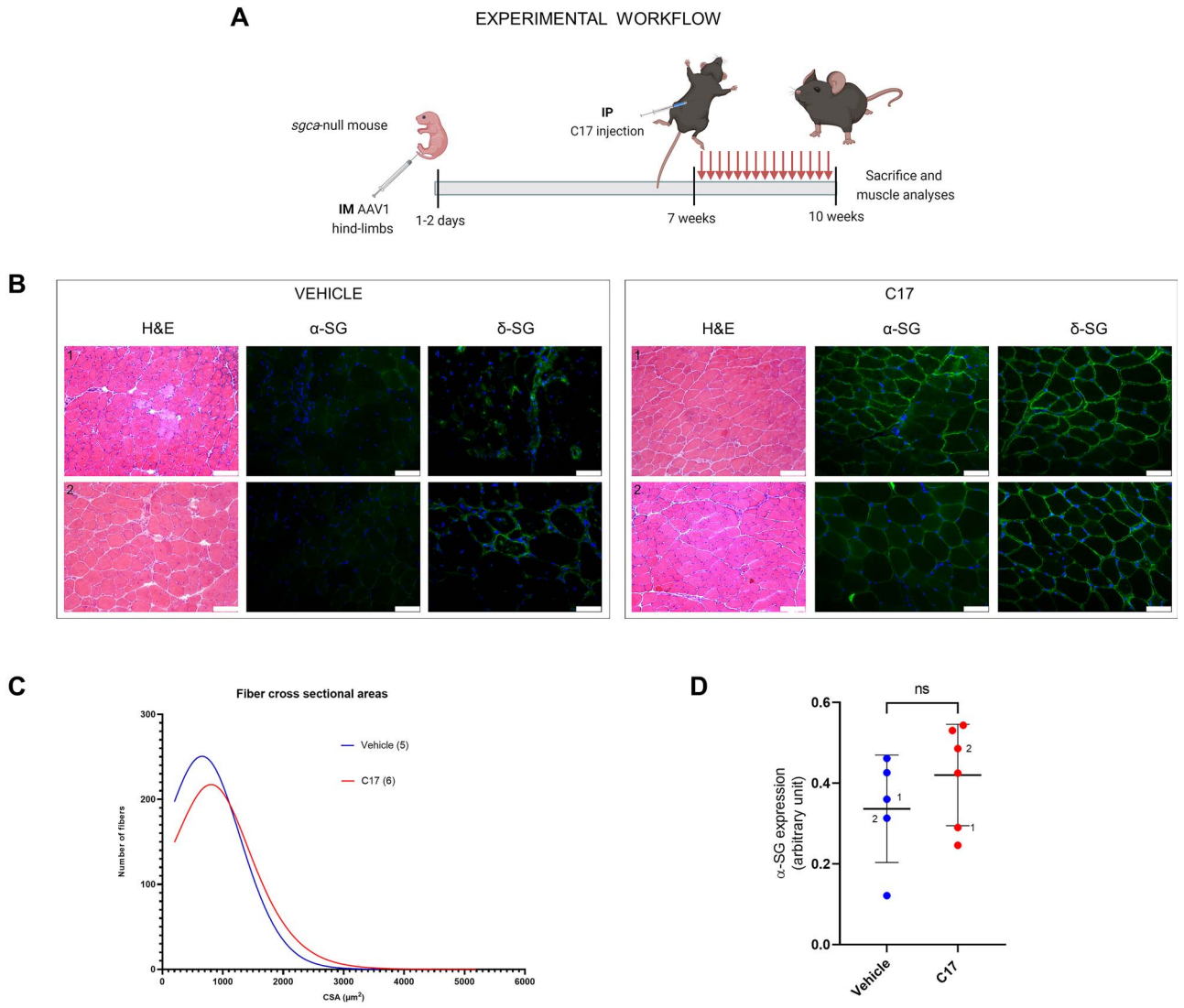

Figure 2. C17 rescued the SG-complex at the sarcolemma of humanized hind-limb muscles. (**A**) Scheme of the experimental work flow (created with BioRender.com). (**B**) H&E staining and IF analysis of representative TA muscle cryo-sections of humanized R98H-α-SG mice treated for 3 weeks with either vehicle or corrector C17. Primary and secondary antibodies like in Fig. 1. Images were captured at the same setting conditions; bars correspond to 100 and 50 μm in H&E and IF images, respectively. (**C**) Graph reporting the distribution of fibers CSA of TA muscles from humanized R98H-α-SG mice treated for 3 weeks with either vehicle (5 samples) or corrector C17 (6 samples). The CSA of an average of 1500 fibers for muscle was measured. (**D**) Densitometric analysis of WB experiments reporting the α-SG expression, normalized for the housekeeping protein GAPDH of vehicle-treated and C17-treated samples. Numbers close to symbols indicate the samples analyzed in B. The graph also reports the mean values ± SD; statistical analysis was performed by unpaired two-tailed Student's *t*-test; ns, $P > 0.05$.

α-SG sequences bearing a single amino acid substitution. Like in human, it is conceivable a slower progression of the disease in comparison to mice lacking the protein (*sgca*-null). As we wanted of dealing with animals in which the disease was established but was still recoverable, we chosen a time interval of 7–12 weeks upon AAV1 injection to analyze the outcome of transduction and of corrector treatments.

The focus on the α-SG V247M mutation was dictated by the fact that it is one of the two variants carried by the myogenic cells used to test CFTR correctors *in vitro* and it is among the most frequently reported missense mutations in LGMDR3 (8,13,14). The R98H mutation was selected as it is associated with a mild/severe phenotype and is classified, such as V247M, as a rescuable mutant by *in vitro* experiments (4–6,13). Conversely, the R77C amino acid substitution was not considered, despite being the most frequently reported mutation in LGMDR3, as the corresponding KI mice failed to develop a dystrophic phenotype (3,15).

As positive control of transduction, we injected the WT sequence of the human α-SG. As expected according to (17,20), the resulting humanized hind-limbs presented a phenotype close to the one of the healthy mice, with the SG-complex residing at the sarcolemma, despite the low amount of the transduced human α-SG (as assessed by WB). This means that mouse tolerated the human protein that assembled into a functional SG-complex with the murine subunits and that it was sufficient one hundredth of the normal amount of α-SG to guarantee the development of a nearly normal phenotype.

The outcome of the transduction with the human V247M-α-SG was the presence of the SG-complex at the sarcolemma and

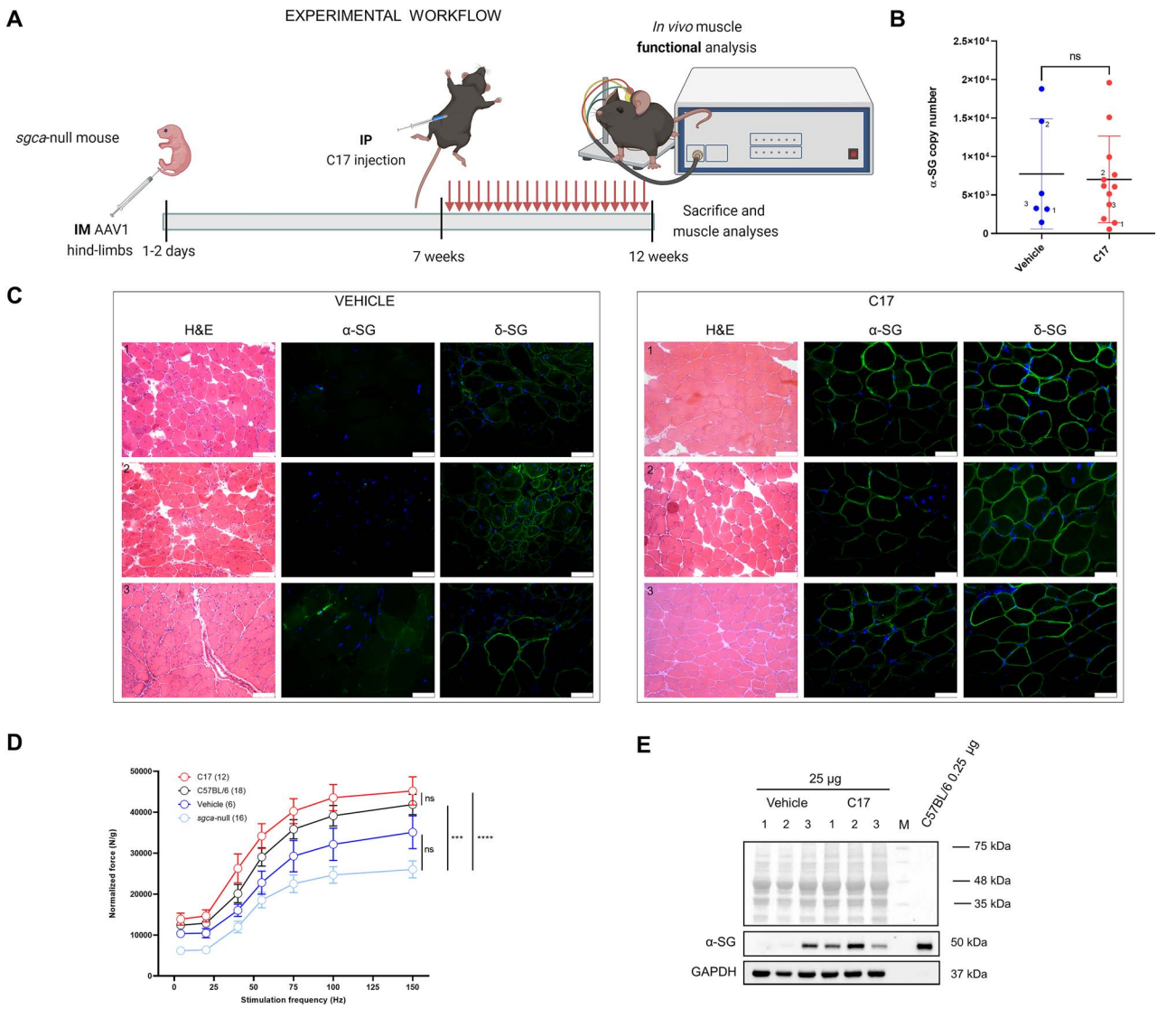

Figure 3. Recovery of the muscle force upon C17 treatment. (**A**) Scheme of the experimental work (created with BioRender.com). (**B**) Evaluation by q-PCR of human α-SG cDNA copy number present in transduced TA muscles at the end of the experiment. The numbers close to symbols indicate the samples analyzed in C and E. The graph also reports the mean values ± SD; statistical analysis was performed by unpaired two-tailed Student's *t*-test; ns, $P \geq 0.05$. (**C**) H&E staining and IF analysis of representative TA muscle cryo-sections of mice expressing the R98H-α-SG treated for 5 weeks with either vehicle or corrector C17. Primary and secondary antibodies like in Fig. 1. Images were captured at the same setting conditions; bars correspond to 100 and 50 μm in H&E and IF images, respectively. (**D**) Force–frequency curves of TA muscle (normalized for muscle weight) elicited by electrical stimulation at the indicated frequencies of WT (positive control), *sgca*-null mice (negative control) and humanized mice treated for 5 weeks with either vehicle or C17 25 mg/kg. Statistical analysis was performed by one-way ANOVA test followed by multiple comparisons Tukey's test; for clarity, statistic symbols are reported for the 150 Hz frequency only. Data are reported as mean values ± SEM. ***, $P \leq 0.001$; ****, $P \leq 0.0001$; ns, $P \geq 0.05$. (**E**) Representative WB of total protein lysates from TA muscle of humanized mice treated for 5 weeks with either vehicle or C17. C57BL/6 TA muscle lysate was used as positive control. Primary and secondary antibodies like in Fig. 1.

the lack of an evident dystrophic phenotype at histological level of the TA muscle. Even though unexpected on the bases of the *in vitro* experiments (4,6,13), this result is in line with the lack of phenotype of SG-KI animals and contributes to strengthen the hypothesis that some difference in the QC system may occur between human and mouse (3,15,16). Furthermore, it is in accordance with the recent genotype–phenotype correlation analysis reporting that LGMDR3 subjects with V247M-α-SG developed a milder disease phenotype with a residual amount of the SG at the sarcolemma higher than 30% (34).

Conversely, when the human R98H-α-SG was transduced, clear myopathic features were present in the TA muscle, with only traces of the mutated protein and a strong reduction of the WT subunits, β-, γ- and δ-SG, at the sarcolemma. This suggests that the QC system efficiently recognized α-SG carrying this mutation that underwent fast degradation, confirming what observed *in vitro* (4,6,13). All this considered, the humanized mouse, novel model of sarcoglycanopathy, is characterized by transient SG expression, even though the transgene may be present up to one year from transduction (17,18). Transgene expression is restricted to the hind-limb muscles and may be affected by the possible different behavior of mouse and human concerning QC and protein degradation. Furthermore, each experiment needs to start with the viral transduction.

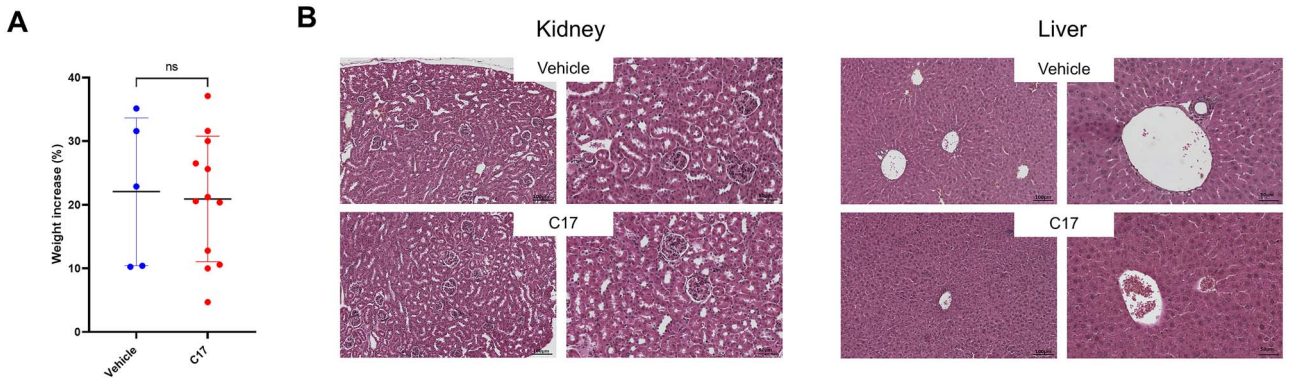

Figure 4. No major toxic effect was observed in humanized mice upon 5 weeks of C17 administration. (**A**) The graph reports the distribution of the body-weight increase of mice at the end of 5 weeks treatment. Mean values ± SD are also indicated. Statistical analysis was performed by unpaired two-tailed Student's t-test; ns, $P > 0.05$. (**B**) H&E staining of fixed kidney (cortex) and liver sections from humanized mice treated with vehicle or C17. Each field is from a different mouse, two magnifications are reported to better appreciate cell-tissue organization.

However, the system is versatile, in principle allowing testing any possible SG mutations in any SG-KO mouse.

As the transduction with the human R98H-α-SG sequence resulted in humanized muscles better mirroring the LGMDR3 condition, we utilized this model for assessing efficacy and safety of corrector C17.

The systemic administration of C17 in humanized animals resulted in a clear amelioration of the myopathic features at the histological level and the rerouting of the SG-complex at the sarcolemma. However, the key finding was the recovery of the muscular function, as assessed *in vivo*. The normalized force produced by TA muscles from C17-treated humanized mice was strongly improved in comparison to the *sgca*-null mice and was almost indistinguishable from that of the WT, healthy animals, proving the efficacy of the CFTR corrector in a model of LGMDR3. Of note, WT mice and C17-treated model animals elicited similar muscle force, even though the total amount of α-SG was remarkably lower in humanized samples, as assessed by WB analysis. Altogether, this suggests that a small amount of protein, as long as it is at the right place (muscle membrane), is the prerequisite for providing sarcolemma protection from damages and preserving muscle activity.

It is also interesting to consider that the muscle force generated by vehicle-treated humanized animals was slightly higher, although not statistically significant, if compared with the negative control animals. We suppose this as the consequence of a minimal escape from degradation of the R98H-α-SG protein that can localize at the sarcolemma together with WT partners. Even though the amount is borderline for detection by IF, it is conceivably enough to assure a partial rescue of muscle force in humanized animals. These data further suggest that α-SG missense mutants are potentially active and their preservation from degradation is *conditio sine qua non* for therapeutic purposes. If the whole process is improved (i.e. by CFTR correctors), the amount of rerouted mutant/SG-complex is sufficient to guarantee full functional recovery.

We also observed that up to 5 weeks of treatment with C17 had no negative effect on growth and behavior of animals. Moreover, liver and kidneys from treated animals presented no substantial differences, both at macro and microscopic level in comparison to the ones from control mice (vehicle). If we consider that liver and kidney are the primary organs involved in metabolism and excretion of pharmacological compounds and that chronic toxicity may alter cell morphology and organ architecture (35–37), the absence of such modifications is a first indication, although not conclusive, that C17 is safe in mouse, at the regimen adopted.

Further experiments are surely needed to definitely exclude toxicity as well as to establish the minimal effective dose and the best ways of administration. However, the present findings, together with data collected with human pathological cells, are proof that a CFTR corrector, specifically C17, may become a therapeutic solution in LGMDR3 (8,13,14). Furthermore, since it was observed that missense mutations behave in similar way independently of the *SGC* gene considered (5), it is predictable the beneficial effect of CFTR correctors in LGMDR4–6 too.

It is clear that sarcoglycanopathies caused by mutations impairing the SG synthesis are not treatable with this approach. However, the sarcoglycanopathy subjects who are homozygotes for frameshift or null mutations represent a minority of all reported cases. Furthermore, compound heterozygosis is frequently reported (8,34,38–42). Thus, considering that a mild disease phenotype seems to correlate with residual amount of SGs at the sarcolemma (34), it is conceivable that the recovery of some quantity of protein, even though from one single allele, should be sufficient to assure the phenotype amelioration. This enlarges the cohort of sarcoglycanopathy patients who could benefit from this pharmacological approach.

Our strategy aims at rescuing the endogenous protein by using small molecules, easy to produce and deliver, and in case to optimize. It is evident the advantage over complex procedures such as gene or cell transfer, without considering patient complains. Furthermore, we are acting on the primary cause of the disease, even though it is well known that secondary events such as inflammation, oxidative stress, etc., are responsible for exacerbating symptoms and accelerating the disease progression (8,39,43). Therefore, to improve the outcome, it is possible to propose combo treatments with drugs aiming at mitigating the secondary events of the muscular dystrophy (44).

In conclusion, our data prove that the activity of a CFTR corrector is not limited to CF but can be extended to sarcoglycanopathies and, theoretically, to other diseases characterized by the presence of a folding-defective, but potentially functional mutant. Even though the path for drug approval is long and studded of difficulties, this *in vivo* proof of concept may be of hope for many patients who, like in LGMDR3, are suffering of an orphan disease.

Materials and Methods

Study design

All *in vivo* experiments were performed in accordance with the European guidelines and regulations for the human care and use of experimental animals. The protocol has been authorized by the Public Veterinary Health Department of the Italian Ministry of Health (Authorization n° 24/2020-PR 10/01/2020).

For the generation and characterization of humanized mice, 1 to 2-day-old *sgca*-null mouse pups were injected in one hind limb with 9×10^9 viral genome (vg) of AAV1 carrying the human α-SG sequence either in the WT form or carrying the R98H or V247M mutation. The contralateral leg was injected with physiological solution as control. Ten weeks upon transduction, mice were sacrificed and the TA muscles explanted for further analyses. Growth and behavior of transduced animals were followed during the entire period.

For small molecule testing, 1 to 2-day-old *sgca*-null mouse pups were injected with AAV1 carrying the human R98H-α-SG sequence in each hind-limb. Seven weeks upon transfection, animals were *intraperitoneally* (IP) injected, daily, with either corrector C17 or vehicle. Three weeks later, animals were sacrificed and muscles of the hind-limbs explanted for biochemical, histological and molecular analyses. Alternatively, after 5 weeks of C17 treatment, the TA muscle force was evaluated *in vivo*, and at the end of the measurements, mice were sacrificed and muscle explanted for biochemical, histological and molecular analyses.

Adeno associated virus production

The R98H or V247M mutation of the human α-SG was introduced in the full-length, tag-less WT sequence cloned in the pcDNA3 vector described in (45) by the subcloning of the BamHI fragments excised from the expressing vectors described in (4). The WT and mutated cDNA sequences were subsequently cloned between the two inverted terminal repeats of the adeno associated virus type 1 (AAV1) vector, under the muscle specific tMCK promoter using the NheI and XhoI sites. All constructs were controlled by DNA sequencing. The cloning process, production and *in vivo*-grade purification of recombinant AAV1 stocks were carried out by the Applied Biological Materials Inc. (Richmond, Canada).

Animal experiments

C57BL/6 and *sgca*-null mice were bred in the animal facility of the Department of Biomedical Sciences, provided with water and food ad libitum and were housed in a thermally controlled room at 20–24°C with a 12-h light/dark cycle. *Sgca*-null mice were previously characterized (33). Both male and female mice were used for this study.

One to two-day-old pups of *sgca*-null mouse were transduced with AAV1 carrying either the WT or mutated (R98H and V247M) human α-SG sequence. Neonate *sgca*-null pups were anesthetized by induced hypothermia; a 30G needle microsyringe was used to deliver intramuscularly the AAV1 particles suspended in phosphate buffer (9×10^{11}-genome copies/ml). Two injections of 5 μL each were performed in the muscles below the knee. After injection, warmed pups returned to their mother, until weaning.

For transduced muscle characterization, 10 weeks upon viral injection, mice were sacrificed by cervical dislocation and muscles of the hind-limbs were explanted and quickly frozen in liquid nitrogen-cooled isopentane.

For drug treatment, 7 weeks upon viral injection, mice were daily injected, intraperitoneally (IP) with either C17 (25 mg/kg) dissolved in 5% DMSO, 5% Kolliphor-EL (46) in physiological solution or vehicle, for 21 or 35 days.

Chemicals

C17 corrector was purchased from Exclusive chemistry (Kaluga region, Obninsk, Russia), Kolliphor-EL and DMSO from Sigma-Aldrich (St. Louis, MO, USA).

Muscle physiology

For *in vivo* force measurement procedure, the animal was deeply anesthetized with an intraperitoneal injection of Ketamine 100 mg/kg Xylazine 10 mg/kg and, a few minutes later, an intramuscular injection of Altadol 5–10 mg/kg as a pain relief treatment. A small incision was made on the side of the knee to the direction of the hip, exposing the common peroneal nerve. A TeflonTM-coated seven-stranded steel wire (AS 632; Cooner Wire Company, Chatsworth, CA, USA) was sutured with 5–0 silk thread at each side of the common peroneal nerve. Upon electrical stimulation, torque production of the TA muscle is measured using a lever system (Model 305B; Aurora Scientific, Aurora, ON, Canada). The electrical stimulation has been performed on a S88 stimulator (Grass Instrument, Warwick, RI, USA) using the following protocol: train duration 200 ms, pulse width 500 μs, 1–2 V and stepwise increase frequencies from a single pulse to 20, 40, 55, 75, 100 and 150 Hz; each train is performed every 30 s to avoid effects due to fatigue.

TA muscles from C57BL/6 and *sgca*-null mice of similar age and weight were used as positive and negative control, respectively. After force measurements, mice were sacrificed by cervical dislocation, and muscles were dissected, weighed and frozen in isopentane precooled in liquid nitrogen for further analyses.

Explant, fixing, paraffine inclusion and slice-preparation of mouse kidney and liver

Immediately upon sacrifice, liver and kidneys were explanted and immersed in 4% buffered neutral paraformaldehyde at 4°C for 48 hours. To promote fixative penetration in the tissue, each liver was cut in 6 pieces and each kidney in 2 pieces. Subsequently, organs were extensively washed with phosphate-buffered saline (PBS, 0.1 M, pH 7.4) and finally immersed in 70% ethanol for conservation and/or further processing. For histological analysis, tissue fragments were de-hydrated through a graded series of ethanol and embedded in paraffin.

Histological, morphometric and IF analyses

From paraffine-embedded livers and kidneys, sections (5-μm thick) were cut in a microtome and were stained with hematoxylin and eosin (H&E). From frozen muscle explants, transverse cross sections (8-μm thick) were cut in a cryostat microtome (Leica CM1850) set at -24 ± 1°C. H&E staining was performed to examine the general morphology of tissues.

To easily determine the CSA of individual muscle fibers, immunostaining was performed using an antibody against laminin to visualize the basal lamina according to (47). Briefly, muscle cryo-sections were blocked with 5% normal goat serum in PBS and subsequently incubated for 1 hour at 37°C with the rabbit polyclonal antibody specific for laminin diluted 1:150 in 5% fetal bovine serum. The primary antibody was revealed with an anti-rabbit Alexa-Fluor-488 diluted 1:200 in PBS incubated for

1 hour at 37°C. Nuclei were counterstained with DAPI (Abcam, Cambridge, UK). Muscle sections were examined with a Leica RD100 fluorescence microscope equipped with a digital camera. Muscle fiber CSA was measured on digital photographs using ImageJ software (Scion, Frederick, MD).

Immunofluorescent staining of α-, β- and δ-SG was carried out to assess the cytolocalization of the proteins. Muscle cryosections were washed and blocked with 10% normal goat serum in 0.5% bovine serum albumin (BSA) in PBS for 1 hour at room temperature. Muscle sections were incubated overnight at 4°C with the primary antibodies (all raised in rabbit) specific for α-, β- and δ-SG diluted, respectively, 1:2000, 1:100 and 1:500 in 0.5% BSA. Protein signals were revealed with an anti-rabbit Alexa-Fluor-488 diluted 1:500 in 0.5% BSA in PBS incubated for 2 hours at room temperature. Nuclei were counterstained with DAPI (Abcam, Cambridge, UK). As negative controls, immunostaining with the sole secondary antibodies was performed. Muscle sections were examined with a Leica DMR fluorescence microscope equipped with a digital camera.

WB analysis

For WB analysis, about 10 mg of TA muscle were incubated in lysis buffer containing 3% SDS, 0.1 mM EGTA supplemented with complete protease inhibitors cocktail, Sigma-Aldrich (St. Louis, MO, USA), and homogenized with the TissueLyser II instrument (Quiagen, Hilden, Germany). Proteins were resolved by SDS-PAGE, blotted onto a nitrocellulose membrane and probed with selected primary antibodies. Secondary antibodies were horseradish peroxidase-conjugated, and blots were developed with ECL chemiluminescent substrate (Genetex, Alton Pkwy Irvine, CA, USA); signals were digitally acquired with Alliance Mini HD9 Imaging System (Uvitec, Cambridge, UK). Densitometry was performed with the ImageJ software. The intensities of sarcoglycan bands were normalized for the intensity of the housekeeping protein GAPDH.

Antibodies

Rabbit monoclonal anti α-SG (AB189254) and rabbit polyclonal anti β-SG (AB83699) were from Abcam (Cambridge, UK); rabbit polyclonal anti GAPDH (G9545) and rabbit polyclonal anti laminin (L9393) were from Sigma-Aldrich (St. Louis, MO, USA); rabbit polyclonal antibody specific for δ-SG was produced and characterized as previously described (6).

WB secondary antibodies were horseradish peroxidase-conjugated goat anti-rabbit IgG (Sigma-Aldrich, St. Louis, MO, USA), while fluorescent antibodies were Alexa Fluor 488-conjugated goat anti-rabbit IgG (Invitrogen, Carlsbad, CA, USA).

Quantitative real-time PCR

Total DNA was extracted from 10 mg of TA muscle with MyTaq Extract-PCR kit (Meridian Bioscience) according to manufacturer's protocol. DNA concentration, upon RNAse treatment, was determined at the Nanodrop 2000 spectrophotometer (Thermo Scientific, Wilmington, DE); 500 ng of each sample were used for the PCR reactions.

Serial 10-fold dilutions starting from 10^9 genome copies/mL of the viral vector were used to prepare the standard curve by plotting the vector copy number logarithm against the measured threshold cycle (Ct) values, as reported in (48). The amount of DNA quantified for each sample was expressed as a number of genome copies per ml.

The PCR parameters were: initial denaturation at 95°C for 10 min followed by 40 cycles of 10 s at 95°C and 30 s at 60°C for acquisition of fluorescence signal. A melting curve was generated by the iQ5 software at the end of the final cycle for each sample to confirm the specificity of the amplified product. The PCR reactions were performed in triplicate in 10 μL final volume in IQ5 Thermal Cycler (Bio-Rad, Hercules, CA, USA) using Biorad iQ Sybr green supermix. Primer sequences were as follows: human α-SG forward primer 5′- CCCCAGACCGTGACTTCTTG-3′, human α-SG reverse primer 5′- TCTCTTCAGCCTTCCCTCCC-3′.

Statistical analysis

Data were expressed as means ± SD. For *in vivo* functional experiments, data were expressed as means ± SEM. Statistical differences among groups were determined by one-way ANOVA test, followed by Tukey's multiple comparisons test. When only two groups were considered, statistical analysis was performed by the unpaired two-tailed Student's t-test. A level of confidence of $P < 0.05$ was used for statistical significance.

Authors' contributions

Author contributions: M.S., A.B., L.N., R.S. Investigation, Methodologies, Formal analysis, Data curation; L.N., M.B., F.D.B., M.S., S.F., E.E.A., P.C., M.C. Investigation, Formal analysis; B.B. Resources, Validation; D.S. M.S. Conceptualization, Validation; D.S. Funding acquisition, Project administration, Supervision, Writing—original draft.

Supplementary Material

Supplementary Material is available at *HMG* online.

Acknowledgements

Authors would like to acknowledge Dr Chiara Fecchio for the valuable help in designing AAV vectors and Mr. Mauro Ghidotti for the valuable help and advices in animal handling. We are grateful to the Cystic Fibrosis Foundation for providing the first stock of CFTR correctors.

Conflict of Interest statement. The authors declare no conflict of interest.

Funding

Association Française contre les Myopathies (AFM#18620, AFM#23000); Italian Telethon Foundation (GGP15140, GGP20097); Muscular Dystrophy Association (MDA 577888).

References

1. Straub, V., Murphy, A., Udd, B. and LGMD Workshop Study Group (2018) 229th ENMC international workshop: limb girdle muscular dystrophies - nomenclature and reformed classification Naarden, the Netherlands, 17-19 march 2017. *Neuromuscul. Disord.*, **28**, 702–710.
2. Tarakci, H. and Berger, J. (2016) The sarcoglycan complex in skeletal muscle. *Front. Biosci. (Landmark Ed)*, **21**, 744–756.
3. Bartoli, M., Gicquel, E., Barrault, L., Soheili, T., Malissen, M., Malissen, B., Vincent-Lacaze, N., Perez, N., Udd, B., Danos, O. *et*

al. (2008) Mannosidase I inhibition rescues the human alpha-sarcoglycan R77C recurrent mutation. *Hum. Mol. Genet*., **17**, 1214–1221.
4. Gastaldello, S., D'Angelo, S., Franzoso, S., Fanin, M., Angelini, C., Betto, R. and Sandona, D. (2008) Inhibition of proteasome activity promotes the correct localization of disease-causing alpha-sarcoglycan mutants in HEK-293 cells constitutively expressing beta-, gamma-, and delta-sarcoglycan. *Am. J. Pathol*., **173**, 170–181.
5. Soheili, T., Gicquel, E., Poupiot, J., N'Guyen, L., Le Roy, F., Bartoli, M. and Richard, I. (2012) Rescue of sarcoglycan mutations by inhibition of endoplasmic reticulum quality control is associated with minimal structural modifications. *Hum. Mutat*., **33**, 429–439.
6. Bianchini, E., Fanin, M., Mamchaoui, K., Betto, R. and Sandona, D. (2014) Unveiling the degradative route of the V247M alpha-sarcoglycan mutant responsible for LGMD-2D. *Hum. Mol. Genet*., **23**, 3746–3758.
7. Sandona, D. and Betto, R. (2009) Sarcoglycanopathies: molecular pathogenesis and therapeutic prospects. *Expert Rev. Mol. Med*., **11**, e28.
8. Carotti, M., Fecchio, C. and Sandona, D. (2017) Emerging therapeutic strategies for sarcoglycanopathy. *Expert Opin. Orphan Drug*, **5**, 381–396.
9. Gelman, M.S., Kannegaard, E.S. and Kopito, R.R. (2002) A principal role for the proteasome in endoplasmic reticulum-associated degradation of misfolded intracellular cystic fibrosis transmembrane conductance regulator. *J. Biol. Chem*., **277**, 11709–11714.
10. Rogan, M.P., Stoltz, D.A. and Hornick, D.B. (2011) Cystic fibrosis transmembrane conductance regulator intracellular processing, trafficking, and opportunities for mutation-specific treatment. *Chest*, **139**, 1480–1490.
11. Mijnders, M., Kleizen, B. and Braakman, I. (2017) Correcting CFTR folding defects by small-molecule correctors to cure cystic fibrosis. *Curr. Opin. Pharmacol*., **34**, 83–90.
12. Lopes-Pacheco, M. (2020) CFTR modulators: the changing face of cystic fibrosis in the era of precision medicine. *Front. Pharmacol*., **10**, 1662–1690.
13. Carotti, M., Marsolier, J., Soardi, M., Bianchini, E., Gomiero, C., Fecchio, C., Henriques, S.F., Betto, R., Sacchetto, R., Richard, I. *et al*. (2018) Repairing folding-defective alpha-sarcoglycan mutants by CFTR correctors, a potential therapy for limb-girdle muscular dystrophy 2D. *Hum. Mol. Genet*., **27**, 969–984.
14. Carotti, M., Scano, M., Fancello, I., Richard, I., Risato, G., Bensalah, M., Soardi, M. and Sandona, D. (2020) Combined use of CFTR correctors in LGMD2D myotubes improves sarcoglycan complex recovery. *Int. J. Mol. Sci*., **21**, 1813–1828.
15. Kobuke, K., Piccolo, F., Garringer, K.W., Moore, S.A., Sweezer, E., Yang, B. and Campbell, K.P. (2008) A common disease-associated missense mutation in alpha-sarcoglycan fails to cause muscular dystrophy in mice. *Hum. Mol. Genet*., **17**, 1201–1213.
16. Henriques, S.F., Patissier, C., Bourg, N., Fecchio, C., Sandona, D., Marsolier, J. and Richard, I. (2018) Different outcome of sarcoglycan missense mutation between human and mouse. *PLoS One*, **13**, e0191274.
17. Pacak, C.A., Walter, G.A., Gaidosh, G., Bryant, N., Lewis, M.A., Germain, S., Mah, C.S., Campbell, K.P. and Byrne, B.J. (2007) Long-term skeletal muscle protection after gene transfer in a mouse model of LGMD-2D. *Mol. Ther*., **15**, 1775–1781.
18. Pacak, C.A., Conlon, T., Mah, C.S. and Byrne, B.J. (2008) Relative persistence of AAV serotype 1 vector genomes in dystrophic muscle. *Genet. Vaccines Ther*., **6**, 14–17.
19. Wang, B., Li, J., Fu, F.H., Chen, C., Zhu, X., Zhou, L., Jiang, X. and Xiao, X. (2008) Construction and analysis of compact muscle-specific promoters for AAV vectors. *Gene Ther*., **15**, 1489–1499.
20. Allamand, V., Donahue, K.M., Straub, V., Davisson, R.L., Davidson, B.L. and Campbell, K.P. (2000) Early adenovirus-mediated gene transfer effectively prevents muscular dystrophy in alpha-sarcoglycan-deficient mice. *Gene Ther*., **7**, 1385–1391.
21. Davison, H.R., Taylor, S., Drake, C., Phuan, P.W., Derichs, N., Yao, C., Jones, E.F., Sutcliffe, J., Verkman, A.S. and Kurth, M.J. (2011) Functional fluorescently labeled bithiazole DeltaF508-CFTR corrector imaged in whole body slices in mice. *Bioconjug. Chem*., **22**, 2593–2599.
22. Al Shoyaib, A., Archie, S.R. and Karamyan, V.T. (2019) Intraperitoneal route of drug administration: should it be used in experimental animal studies? *Pharm. Res*., **37**, 12–28.
23. Shi, W., Chen, Z., Schottenfeld, J., Stahl, R.C., Kunkel, L.M. and Chan, Y.M. (2004) Specific assembly pathway of sarcoglycans is dependent on beta- and delta-sarcoglycan. *Muscle Nerve*, **29**, 409–419.
24. Draviam, R.A., Shand, S.H. and Watkins, S.C. (2006) The beta-delta-core of sarcoglycan is essential for deposition at the plasma membrane. *Muscle Nerve*, **34**, 691–701.
25. Allikian, M.J. and McNally, E.M. (2007) Processing and assembly of the dystrophin glycoprotein complex. *Traffic*, **8**, 177–183.
26. Rossi, C.A., Flaibani, M., Blaauw, B., Pozzobon, M., Figallo, E., Reggiani, C., Vitiello, L., Elvassore, N. and De Coppi, P. (2011) *In vivo* tissue engineering of functional skeletal muscle by freshly isolated satellite cells embedded in a photopolymerizable hydrogel. *FASEB J*., **25**, 2296–2304.
27. Blaauw, B., Agatea, L., Toniolo, L., Canato, M., Quarta, M., Dyar, K.A., Danieli-Betto, D., Betto, R., Schiaffino, S. and Reggiani, C. (2010) Eccentric contractions lead to myofibrillar dysfunction in muscular dystrophy. *J. Appl. Physiol*., **108**, 105–111.
28. Birault, V., Solari, R., Hanrahan, J. and Thomas, D.Y. (2013) Correctors of the basic trafficking defect of the mutant F508del-CFTR that causes cystic fibrosis. *Curr. Opin. Chem. Biol*., **17**, 353–360.
29. Sampson, H.M., Lam, H., Chen, P.C., Zhang, D.L., Mottillo, C., Mirza, M., Qasim, K., Shrier, A., Shyng, S.L., Hanrahan, J.W. *et al*. (2013) Compounds that correct F508del-CFTR trafficking can also correct other protein trafficking diseases: an *in vitro* study using cell lines. *Orphanet J. Rare Dis*., **8**, 11–22.
30. Sabirzhanova, I., Pacheco, M.L., Rapino, D., Grover, R., Handa, J.T., Guggino, W.B. and Cebotaru, L. (2015) Rescuing trafficking mutants of the ATP-binding cassette protein, ABCA4, with small molecule correctors as a treatment for stargardt eye disease. *J. Biol. Chem*., **290**, 19743–19755.
31. van der Woerd, W.L., Wichers, C.G.K., Vestergaard, A.L., Andersen, J.P., Paulusma, C.C., Houwen, R.H.J. and van de Graaf, S.F.J. (2016) Rescue of defective ATP8B1 trafficking by CFTR correctors as a therapeutic strategy for familial intrahepatic cholestasis. *J. Hepatol*., **64**, 1339–1347.
32. Duclos, F., Straub, V., Moore, S.A., Venzke, D.P., Hrstka, R.F., Crosbie, R.H., Durbeej, M., Lebakken, C.S., Ettinger, A.J., van der Meulen, J. *et al*. (1998) Progressive muscular dystrophy in alpha-sarcoglycan-deficient mice. *J. Cell Biol*., **142**, 1461–1471.
33. Liu, L.A. and Engvall, E. (1999) Sarcoglycan isoforms in skeletal muscle. *J. Biol. Chem*., **274**, 38171–38176.

34. Alonso-Perez, J., Gonzalez-Quereda, L., Bello, L., Guglieri, M., Straub, V., Gallano, P., Semplicini, C., Pegoraro, E., Zangaro, V., Nascimento, A. *et al.* (2020) New genotype-phenotype correlations in a large European cohort of patients with sarcoglycanopathy. *Brain*, **143**, 2696–2708.
35. Ramachandran, R. and Kakar, S. (2009) Histological patterns in drug-induced liver disease. *J. Clin. Pathol.*, **62**, 481–492.
36. Kleiner, D.E. (2018) Recent advances in the histopathology of drug-induced liver injury. *Surg. Pathol. Clin.*, **11**, 297–311.
37. John, R. and Herzenberg, A.M. (2009) Renal toxicity of therapeutic drugs. *J. Clin. Pathol.*, **62**, 505–515.
38. Guglieri, M., Magri, F., D'Angelo, M.G., Prelle, A., Morandi, L., Rodolico, C., Cagliani, R., Mora, M., Fortunato, F., Bordoni, A. *et al.* (2008) Clinical, molecular, and protein correlations in a large sample of genetically diagnosed Italian limb girdle muscular dystrophy patients. *Hum. Mutat.*, **29**, 258–266.
39. Angelini, C. and Fanin, M. (2016) Pathogenesis, clinical features and diagnosis of sarcoglycanopathies. *Expert Opin. Orphan Drugs*, **4**, 1239–1251.
40. Fanin, M., Nascimbeni, A.C., Aurino, S., Tasca, E., Pegoraro, E., Nigro, V. and Angelini, C. (2009) Frequency of LGMD gene mutations in Italian patients with distinct clinical phenotypes. *Neurology*, **72**, 1432–1435.
41. Ginjaar, H.B., van der Kooi, A.J., Ceelie, H., Kneppers, A.L., van Meegen, M., Barth, P.G., Busch, H.F., Wokke, J.H., Anderson, L.V., Bonnemann, C.G. *et al.* (2000) Sarcoglycanopathies in Dutch patients with autosomal recessive limb girdle muscular dystrophy. *J. Neurol.*, **247**, 524–529.
42. Mahmood, O.A., Jiang, X. and Zhang, Q. (2013) Limb-girdle muscular dystrophy subtypes: first-reported cohort from northeastern China. *Neural Regen. Res.*, **8**, 1907–1918.
43. Kirschner, J. and Lochmuller, H. (2011) Sarcoglycanopathies. *Handb. Clin. Neurol.*, **101**, 41–46.
44. Careccia, G., Saclier, M., Tirone, M., Ruggieri, E., Principi, E., Raffaghello, L., Torchio, S., Recchia, D., Canepari, M., Gorzanelli, A. *et al.* (2021) Rebalancing expression of HMGB1 redox isoforms to counteract muscular dystrophy. *Sci. Transl. Med.*, **13**, eaay8416.
45. Sandona, D., Gastaldello, S., Martinello, T. and Betto, R. (2004) Characterization of the ATP-hydrolysing activity of alpha-sarcoglycan. *Biochem. J.*, **381**, 105–112.
46. Aronson JK. (2016) Meyler's Side Effects of Drugs: *The International Encyclopedia of Adverse Drug Reactions and Interactions*. 16th ed. Elsevier, Amsterdam, the Netherlands, pp. 866–867.
47. Mouisel, E., Vignaud, A., Hourde, C., Butler-Browne, G. and Ferry, A. (2010) Muscle weakness and atrophy are associated with decreased regenerative capacity and changes in mTOR signaling in skeletal muscles of venerable (18-24-month-old) dystrophic mdx mice. *Muscle Nerve*, **41**, 809–818.
48. Cui, X., Shi, Y., Zhao, L., Gu, S., Wei, C., Yang, Y., Wen, S., Chen, H. and Ge, J. (2018) Application of real-time quantitative PCR to detect mink circovirus in naturally and experimentally infected minks. *Front. Microbiol.*, **9**, 937–944.